Environmental conditions framing the first evidence of modern humans at Tam Pà Ling, Laos: A stable isotope record from terrestrial gastropod carbonates

Stefania Milano, Fabrice Demeter, Jean-Jacques Hublin, Philippe Duringer, Elise Patole-Edoumba, Jean-Luc Ponche, Laura Shackelford, Quentin Boesch, Nguyen Thi Mai Houng, Luu Thi Phoung Lan, et al.

Palaeogeography, Palaeoclimatology, Palaeoecology 511 (2018) 352–363

Contents lists available at ScienceDirect

Palaeogeography, Palaeoclimatology, Palaeoecology

journal homepage: www.elsevier.com/locate/palaeo

Environmental conditions framing the first evidence of modern humans at Tam Pà Ling, Laos: A stable isotope record from terrestrial gastropod carbonates

Stefania Milano[a,*], Fabrice Demeter[b,c], Jean-Jacques Hublin[a], Philippe Duringer[d], Elise Patole-Edoumba[e], Jean-Luc Ponche[f], Laura Shackelford[g], Quentin Boesch[d], Nguyen Thi Mai Houng[h], Luu Thi Phoung Lan[i], Somoh Duangthongchit[j], Thongsa Sayavonkhamdy[j], Phonephanh Sichanthongtip[j], Daovee Sihanam[j], Viengkeo Souksavatdy[j], Kira Westaway[k], Anne-Marie Bacon[l]

[a] Department of Human Evolution, Max Planck Institute for Evolutionary Anthropology, Deutscher Platz 6, 04103 Leipzig, Germany
[b] Center for GeoGenetics, Øster Voldgade 5-7, 1350 Copenhagen K, Denmark
[c] UMR7206, Musée de l'Homme, 17 Place du Trocadéro, 75116 Paris, France
[d] Ecole et Observatoire des Sciences de la Terre (EOST), Institut de Physique du Globe de Strasbourg (IPGS), UMR 7516 CNRS, Université de Strasbourg, 1 rue Blessig, 67084 Strasbourg Cedex, France
[e] Muséum d'histoire naturelle, 28 rue Albert Ier, 17000 La Rochelle, France
[f] Laboratoire Image Ville et Environnement, UMR 7362, Institut de Géologie, 1 rue Blessig, 67084 Strasbourg Cedex, France
[g] Department of Anthropology, University of Illinois at Urbana-Champaign, Urbana, IL 61801, USA
[h] Anthropological and Palaeoenvironmental Department, The Institute of Archaeology, 61 Phan Chu Trinh, Hanoi, Viet Nam
[i] Institute of Geophysics, Vietnam Academy of Science and Technology, A8, 18 Hoang Quoc Viet, Cau Giay, Hanoi, Viet Nam
[j] Department of Heritage, Ministry of Information, Culture and Tourism, Lao Democratic People's Republic
[k] 'Traps' MQ Luminescence Dating Facility, Dept Environmental Sciences, Macquarie University, Sydney, NSW 2109, Australia
[l] AMIS Anthropologie moléculaire et imagerie de synthèse, UMR 5288 CNRS, Université Paris Descartes, Faculté de chirurgie dentaire, 1 rue Maurice Arnoux, 92120 Montrouge, France

ARTICLE INFO

Keywords:
Paleoenvironment
Land snails
Oxygen and carbon stable isotopes
Late Pleistocene

ABSTRACT

Mainland Southeast Asia is a key region to interpret modern human migrations; however, due to a scarcity of terrestrial proxies, environmental conditions are not well understood. This study focuses on the Tam Pà Ling cave site in northeast Laos, which contains the oldest evidence for modern humans in Indochina, dating back to MIS 4 (70 ± 8 ka). Snail remains of *Camaena massiei* found throughout the stratigraphic sequence contain a valuable oxygen and carbon isotope record of past local vegetation and humidity changes. Our data indicate that before the Last Glacial Maximum (LGM), northeast Laos was characterized by a humid climate and forested environments. With the onset of the LGM, a major climatic shift occurred, inducing a sharp decrease in precipitation and a significant decline in woodland habitats in favor of the expansion to more open landscapes. Only during the Holocene did forests return in northeast Laos, resembling present conditions. The first *Homo sapiens* arriving in Indochina therefore encountered landscapes dominated by woodlands with a minor proportion of open habitats.

1. Introduction

The earliest evidence of modern human dispersal out of Africa has been recently dated between 177 and 194 ka, based on the finding of a maxilla from Misliya Cave, Israel (Hershkovitz et al., 2018). These results pre-date the presence of *Homo sapiens* in the Levantine, previously dated around 90–120 ka (Schwarcz et al., 1988; Mercier et al., 1993). However, numerous uncertainties still exist concerning the arrival of modern humans in East Asia. Some of the oldest fossils were found in Daoxian, Southern China and they were dated 120–80 ka (Liu et al., 2015). Nevertheless, incomplete geochronological and taphonomical information considerably limit the legitimacy of these findings (Michel

* Corresponding author.
E-mail address: stefania_milano@eva.mpg.de (S. Milano).

https://doi.org/10.1016/j.palaeo.2018.08.020
Received 28 June 2018; Received in revised form 29 August 2018; Accepted 31 August 2018
Available online 05 September 2018

et al., 2016). In the Southeast of Asia, more remains were excavated from East Java in association with a fauna assemblage dated between 128 ± 15 and 118 ± 3 ka (Storm and De Vos, 2006; Westaway et al., 2007). According to Badoux (1959), five hominid teeth were excavated but they were subsequently lost and could not be found again in the collection. Another tooth was recovered from the assemblage and it was attributed to *Homo sapiens* (Storm et al., 2005). Recently, more *H. sapiens* teeth were excavated from Lida Ajer cave in Sumatra dating between 73 and 63 ka (Westaway et al., 2017). To date, they represent the first and most robust evidence of modern humans in the insular Southeast Asian rainforests, implying an early arrival in this region before 60 ka (Westaway et al., 2017).

Strong support for this early movement hypothesis derives from the *H. sapiens* material excavated from Tam Pà Ling cave in northeast Laos dated 70 ± 8 ka. A partial cranium with almost complete upper dentition (TPL1), two mandibles (TPL2, TPL3), a rib (TPL4) and a pedal phalanx (TPL5) were excavated from stratigraphic layers in an age range of 46–70 ka (OSL and pIR-IRSL), with a maximum depositional age of 70 ± 8 ka (pIR-IRSL) (Demeter et al., 2012; Demeter et al., 2017; Shackelford et al., 2018). These findings confirm the presence of modern humans in mainland Southeast Asia during MIS 4, supporting the hypothesis that eastward movements beyond Africa may have started during MIS 5 (Boivin et al., 2013). In this humid phase, arid areas such as Arabia and Thar deserts would be minimized allowing growth of patches of edible vegetation together with numerous riverine and lake systems to function as dispersal corridors (Petraglia et al., 2010; Blinkhorn et al., 2013). Further expansion toward Southeast Asia was suggested to have occurred by movements along coastal corridors (Stringer, 2000; Bulbeck, 2007). However, evidence of human presence in continental areas such as in Tam Pà Ling cave (~270 km inland), together with the high instability characterizing coastal environments during the Late Pleistocene may indicate alternative routes (Westley and Dix, 2006; Shackelford et al., 2018).

As for the migration out of Africa, the climatic conditions may have played a major role in movements and early settlements in Southeast Asia. However, this relationship is far from understood due to a scarcity of terrestrial paleoclimate records in this region (Penny, 2001). To better understand the possible role of the environment in colonization of this area of the world, more local paleoenvironmental data are needed. The present study aims to interpret the environmental conditions existing at the time of the first arrival of modern humans in Indochina by reconstructing vegetation distribution (C_3, trees and temperate-climate grasses versus C_4, tropical and subtropical grasses) and humidity levels in northeastern Laos during the last ~70 ka. The archive used to address this research question consists of terrestrial mollusk shells excavated from the Tam Pà Ling cave.

2. Background

During the formation and growth of their calcium carbonate shells, mollusks record crucial information on the surrounding environment such as changes in water temperature, salinity levels (marine species) and precipitation and vegetation patterns (terrestrial species; Rhoads and Pannella, 1970; Jones, 1983). For this reason, they are being increasingly used in paleoclimatic studies (Schöne et al., 2005; Butler et al., 2013; Reynolds et al., 2016). The environmental signatures can be encoded in the form of geochemical and physical properties in the shell (Milano et al., 2017). Among the existing proxies, oxygen and carbon stable isotope ratio ($\delta^{18}O$ and $\delta^{13}C$, respectively) are the most well-established (Leng and Lewis, 2016). Terrestrial snails have a high preservation potential, especially in deposits forming in low-energy environments such as loess, paleosol and tufa (Rousseau, 2001; Antoine and Limondin-Lozouet, 2004; Marković et al., 2006). Malacological remains from archaeological contexts have been used to infer information on human-environment interactions in different parts of the world such as the Mediterranean (i.e. Bonadonna and Leone, 1995; Colonese et al., 2010; Prendergast et al., 2016), the Americas (i.e. Bonadonna et al., 1999; Balakrishnan et al., 2005; Yanes et al., 2014) and Africa (Leng et al., 1998).

In terrestrial pulmonate snails, the major source of oxygen is the water assimilated through the integument (Prior, 1985). Relative to meteoric water $\delta^{18}O$, the $\delta^{18}O$ in snail body fluids is slightly more positive due to evaporative and physiological processes (Balakrishnan and Yapp, 2004). In equilibrium with these fluids, the shell carbonate is precipitated, recording the environmental conditions and therefore allowing the use of the shells as paleoarchives (Yapp, 1979; Zanchetta et al., 2005). Tracing variability of rainfall $\delta^{18}O$ through shell carbonate geochemistry can reveal information on precipitation patterns. Oxygen isotopic composition of rainwater depends on several factors such as latitude, altitude, distance from the coast and temperature (Dansgaard, 1964). In particular, at low latitudes the major driver of rainfall $\delta^{18}O$ variability is the amount of precipitation (known as “Amount Effect”). For instance, large amounts of precipitation induce a depletion of heavy isotopes and therefore a more negative $\delta^{18}O$ signature, which is reflected in negative shell $\delta^{18}O$ values (Dansgaard, 1964; Rozanski et al., 1993; Araguás-Araguás et al., 1998). For this reason mollusk shell $\delta^{18}O$ variability can be interpreted as proxy for identifying wet and dry climates.

As with oxygen, shell carbon stable isotopes ($\delta^{13}C$) hold information on the environmental conditions at time of shell deposition. The main source of the carbon incorporated into the biogenic mineral derives from the diet (Stott, 2002; Metref et al., 2003). Nevertheless, the $\delta^{13}C$ signature of terrestrial gastropods has been shown to be also partially influenced by the ingestion of carbonate-rich soils (Goodfriend and Stipp, 1983; Goodfriend and Ellis, 2002). The incorporation of soil-derived carbonates may account up to 30% of the snail diet, in particular in regions characterized by carbonate-rich sediments leading to more positive shell $\delta^{13}C$ values (Goodfriend, 1999; Goodfriend and Ellis, 2002; Yanes et al., 2008). However, the response is highly species-specific, with numerous recorded cases of pulmonate snail shells not being significantly influenced by the assimilation of foreign carbonates (Stott, 2002; Chiba and Davison, 2009). Previous studies indicate that the signal derived by the potential assimilation of soil carbonate is overwritten by the carbonate incorporation through diet (Yanes et al., 2008, Yanes and Fernández-Lopez-de-Pablo, 2017). Shell $\delta^{13}C$ results depleted or enriched, according to the type of vegetation ingested by the animal. Because different photosynthetic pathways discriminate in different ways against ^{13}C, carbon isotopes undergo specific fractionations in different type of plants. For instance, C_3 plants are characterized by low $\delta^{13}C$ values, between −37‰ and −20‰ with an average value of −27‰, whereas C_4 plants have more positive values between −17‰ and −10‰ with an average value of −12.5‰ (Kohn, 2010). Plants characterized by C_4 photosynthetic pathways are mainly grasses and sedges. About 93% of all C_4 plants belong to five families (Poaceae, Cyperaceae, Chenopodiaceae, Amaranthaceae, and Euphorbiaceae) which do not include any woody arboreal species (Sage et al., 1999). At low latitudes C_3 and C_4 plants coexist in different proportions according to different environmental factors, i.e. water availability, altitude and light intensity. In open habitats such as tropical savannas have a high representation of C_4 grasses (> 90%), whereas more shaded environments with higher water abundance favor C_3 vegetation (Sage et al., 1999; Sage, 2004; Bond, 2008). By analyzing snail diet composition it is possible to reconstruct the distribution of C_3 and C_4 plants at local scale and therefore infer specific information on the landscapes (Goodfriend, 1988; Yanes et al., 2011).

3. Materials and methods

3.1. Archaeological context

Tam Pà Ling cave (TPL) is located in the Hua Pan province, in northeastern Laos (20°12′31.4″ N, 103°24′35.2″ E) (Fig. 1A). The cave

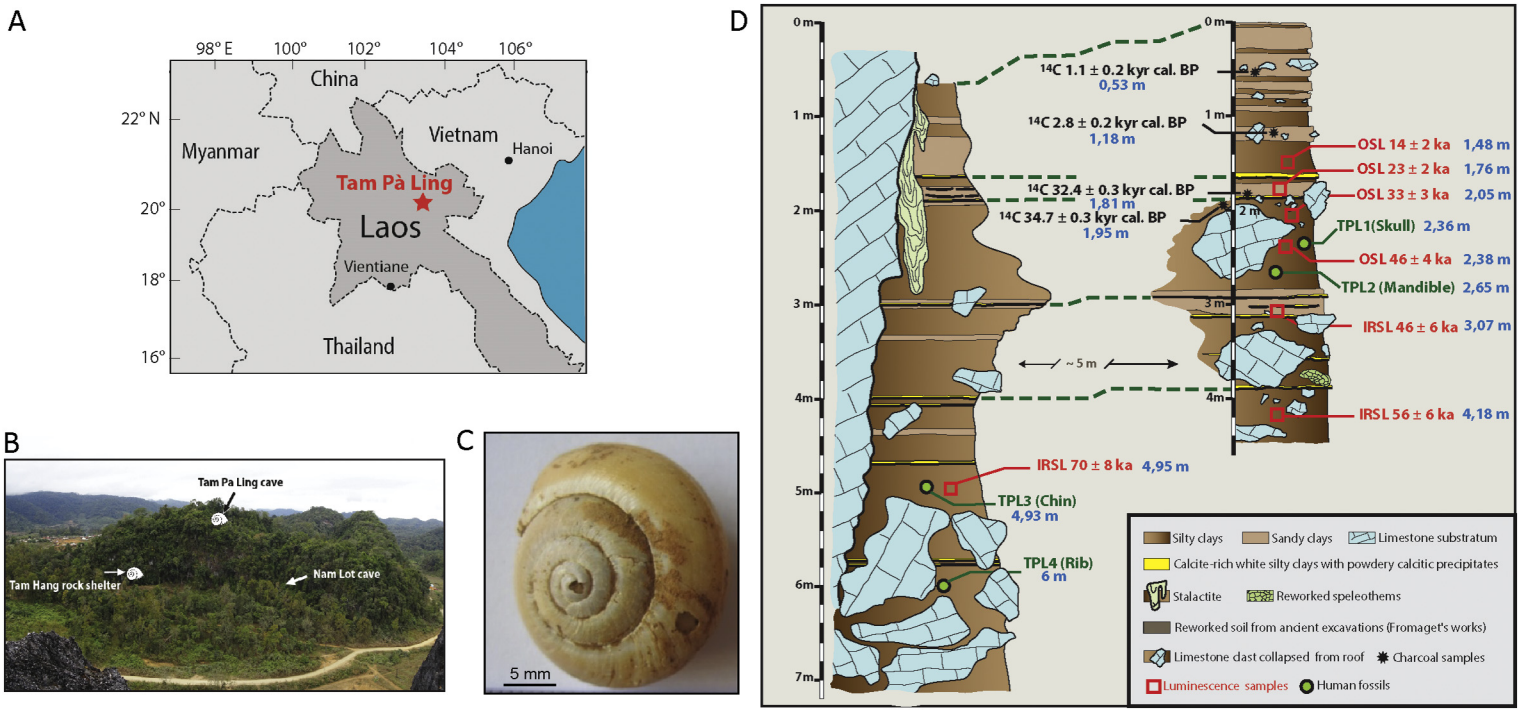

Fig. 1. Details of Tam Pà Ling cave, Laos and its shell material. (A) Location of the cave. (B) View of Tam Pà Ling cave showing the locations of the archaeological and modern shell collections, respectively Tam Pà Ling cave and Tam Hang rock shelter. (C) *Camaena massiei* shell. (D) Stratigraphic sequence of Tam Pà Ling cave (Demeter et al., 2012; Shackelford et al., 2018).

Table 1
Summary of the modern and archaeological shells analyzed in the present study. For details, refer to SI 1.

Time class	Age (ka)	No. of shells analyzed
T0	Modern	3
T1, T2	0.9–3	9
T3	12–16	5
T4	21–25	4
T5, T6, T7	32–36	10
T8, T9	42–52	17
T10	50–62	3
T11	62–78	1

is found at the top of the Pa Hang hill, at an elevation of 1170 m and it is part of the Annamite mountain range, a system of mountains and plateaus bordering the eastern Mekong Basin from northern Laos to the South China Sea (Gupta, 2009). Near TPL, the topography is characterized by rugged hills ranging between 400 and 2000 m in elevation. The geology includes Upper Carboniferous to Permian limestone formations shaped into karst and characterized by numerous caves and galleries (Duringer et al., 2012). The first excavations in the region were conducted in the late 1930s by the geologist Jacques Fromaget who discovered the site of Tam Hang (Fromaget, 1936, 1937, 1940). After > 60 years, in 2003, the research at this location was resumed (Bacon et al., 2008, 2011; Demeter et al., 2009). During further surveys in the area, TPL was discovered in 2008 and it was excavated from 2009 onwards (Demeter et al., 2012, 2015). The cave is formed by one main chamber of 40 × 30 m (W × L). At the entrance a steep slope descends for 65 m toward the chamber floor. The excavated trench (12 × 4 m) lies at the base of this slope. The deposit is made by brown silty to sandy clays. The sediment is wet and soft similar to modeling clays. The proportion of limestone clasts collapsed from the roof or from the entrance of the cave is increasing from top to base of the slope. The stratigraphy indicates that the site was formed by periodic slope washes from the argillaceous sediment bank at the cave entrance (Demeter et al., 2012, 2015). The skull (TPL1), the two mandibles (TPL2, TPL3), the rib (TPL4) and the phalanx (TPL5) were found at different depths in an age range of 46–70 ka (Fig. 1B). Further details about the site and dating can be found in Shackelford et al. (2018).

3.2. Materials and geological context

This study focuses on specimens of the snail *Camaena massiei* (Morlet, 1891) also known as *Helix massiei* (Morlet, 1891) (Fig. 1C). The ecology of this species is not well-known. Although a study specifically focused on *C. massiei* would be needed, basic information on its life cycle and behavior can be inferred from observations at family level and from studies on closely related species. *C. massiei* belongs to the helicoid family Camaenidae with a bi-hemispherical distribution in South-East Asia and America (Wurtz, 1955; Scott, 1996). Species in this family were recorded to have minimum lifespan of 7–8 years (Solem and Christensen, 1984). Adult shell size is usually reached during the animal's second wet season, indicating the occurrence of an ontogenetic decrease of shell deposition with age. Cases of aestivation were recorded during the dry season in Northern Australia (Solem and Christensen, 1984). However, in tropical and subtropical habitats characterized by high humidity levels such as Northern Laos (annual relative humidity above 75%), land snail aestivation is less common (Yanes and Fernández-Lopez-de-Pablo, 2017). Furthermore, a three-year controlled experiment was previously performed on the closely related species *Camaena cicatricosa*, abundant in South China and Vietnam (Xiao, 1989). The results of this study showed that *C. cicatricosa* is an herbivore generalist feeder with a varied diet of fresh vegetables, grass and tree leaves. As many other pulmonate species, these snails are generally more active at night and during humid phases. During the months from November to January the snails tend to be less active but rare cases of aestivation were recorded (Xiao, 1989).

Forty-nine archaeological shells were collected from TPL during the excavation seasons from 2010 to 2016. Their positions through the stratigraphic sequence are given in the Supplementary information (SI 1). Three modern *C. massiei* shells were used as calibration. They were collected in December 2017 from the forest of the Pà Hang Mountain nearby the Tam Hang rock shelter, 50 m below Tam Pà Ling cave.

The age groups of the fossil shells have been defined using the eleven chronological data sets previously obtained from the stratigraphic section, based on samples of charcoal for ^{14}C and soils for OSL and TL dating (Demeter et al., 2017; Shackelford et al., 2018). Using the depth corresponding to each chronological data point as reference, the section was divided into eleven intervals. According to the position of the shells, each of them was assigned to one of these specific intervals and therefore to a specific time class (T1 to T11; Table 1 and SI 1). To provide an accurate division, each spatial interval was split into two subintervals. If the shell was located in the upper half of the interval between two chronological data points, it was assigned to the upper time class and vice versa. Based on this first classification, the eleven time classes were subsequently arranged in seven groups based on similarities in age (SI 1).

3.3. Modern environmental conditions

Monthly air temperature, precipitation and relative humidity data were sourced from a local meteorological station located in Xam Nua (ca 70 km away from TPL; Fig. 2). Rainfall $\delta^{18}O$ values were reported upon calculation using the Online Isotope in Precipitation Calculator (OIPC version 3.1; www.waterisotopes.org). The algorithm on which OIPC runs was developed by Bowen and Wilkinson (2002) to estimate rainfall $\delta^{18}O$ based on a large dataset of direct monthly measurements from almost 400 precipitation-monitoring stations around the world (GNIP).

Considering the habitat range of C3 and C4 plants together with the location of Tam Pa Ling and observations during the excavations, we can derive that the landscape around Tam Pa Ling is dominated by

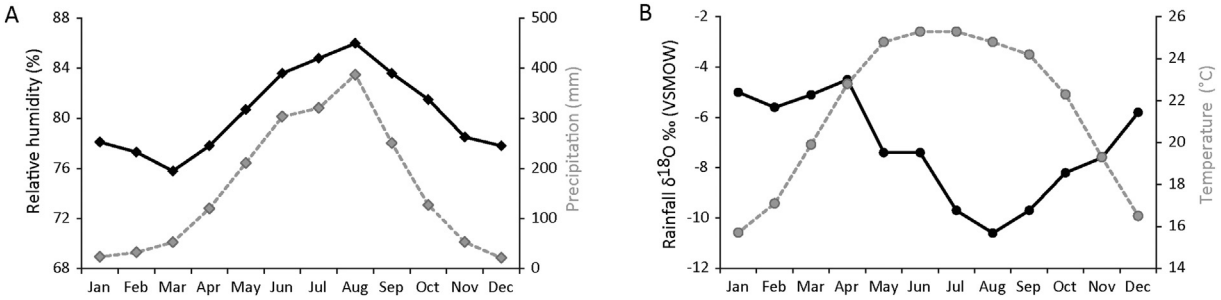

Fig. 2. Modern environmental parameters of Tam Pà Ling region. (A) Monthly fluctuations of relative humidity (black solid line) and precipitation (grey dotted line). (B) Temperature (grey dotted line) and rainfall $\delta^{18}O$ (black solid line) changes throughout the year.

arboreal woody vegetation (mainly C3) interspersed with more open habitats where C4 plants (grasses and shrubs) prevail. In order to quantitatively describe the modern vegetation distribution around Tam Pà Ling, a land cover classification map based on remote sensing was used. This approach allows the characterization of the land surfaces according to the presence of forested versus grassland areas based on multi-band raster images. Satellite images, with a 20 m spatial resolution, were obtained from satellite Sentinel-2A (sensing orbit number 61) on 08th December 2016. The images were analyzed using the image processing and land cover mapping software IMPACT Toolbox (version 3.9 beta; Simonetti et al., 2015). Atmospheric corrections were applied and the satellite images were converted into top-of-atmosphere reflectance. Spectral band 2 (398.6–594.6 nm), 3 (515–605 nm), 4 (626.5–702.5 nm), 8 (690.1–980.1 nm), 11 (1470.7–1756.7 nm) and 12 (1960.4–2444.4 nm) were selected, and the composite image was projected using the Universal Transverse Mercator coordinate system. Image enhancement based on Linear Spectral Unmixing followed by K-means unsupervised classification generated a composite image with 10 spectral classes. Spectral classes were assigned to land cover classes following the comparison with high-spatially resolved satellite images available from Google Earth. Four land cover classes were designed: grassland, mixed grass and shrub, woodland and build-up (Fig. 3).

3.4. Shell preparation and stable isotope measurements

To avoid any contamination by residual organic matter, all shells were ultrasonically rinsed in deionized water for about 10–15 min, cleaned in 10 vol% sodium hypochlorite overnight and rinsed again. After being air-dried, the samples were crushed into powder using an agate mortar and pestle.

The mineralogical phase of the archaeological shells was determined using FTIR (Fourier-transform infrared spectroscopy) to rule out the presence of secondary calcite forming during diagenesis (Fig. 4). As validation, two modern shells were analyzed and compared with the fossil ones. For each sample, a small quantity of shell powder was mixed with ca 40 mg of IR grade KBr and pressed into a pellet using a Wasserman Dental hydraulic press. The analyses were performed with an Agilent 660 FTIR Spectrometer (Agilent Technologies) in transmission mode with a DTGS detector and a 4 cm^{-1} resolution. Each spectrum represented the average of 32 single scans between 4000 and 400 cm^{-1} using Resolution Pro software (Agilent Technologies).

The carbon and oxygen stable isotopes were measured using a Kiel IV automated carbonate preparation device coupled to a Thermo Fisher 253 Plus gas source isotope ratio mass spectrometer at the Department of Human Evolution, Max Planck Institute for Evolutionary Anthropology. The isotope ratios were reported in per mil (‰) relative to the Vienna Pee-Dee Belemnite (VPDB) standard based on IAEA-603 calibrated Carrara marble ($\delta^{18}O = -1.64‰$; $\delta^{13}C = +1.87‰$). The average precision (1σ) determined from replicate analyses was better than 0.05‰ for both $\delta^{18}O$ and $\delta^{13}C$.

The results of the experimental study by Stott (2002) were used to calculate the predicted shell $\delta^{13}C$ according to the snail diet. The model is based on the linear relationship between shell $\delta^{13}C$ and food $\delta^{13}C$ expressed by the following equation:

$$\delta^{13}C_{shell} = \delta^{13}C_{food} \times 0.73889 + 8.666$$

According to this model, a diet consisting only on the ingestion of C_3 plants would lead to a shell $\delta^{13}C$ average value of −11.3‰, whereas a C_4–based diet would result in a shell $\delta^{13}C$ value of −0.6‰. To calculate the effect of the different dietary contributions of C_3 and C_4 plants on

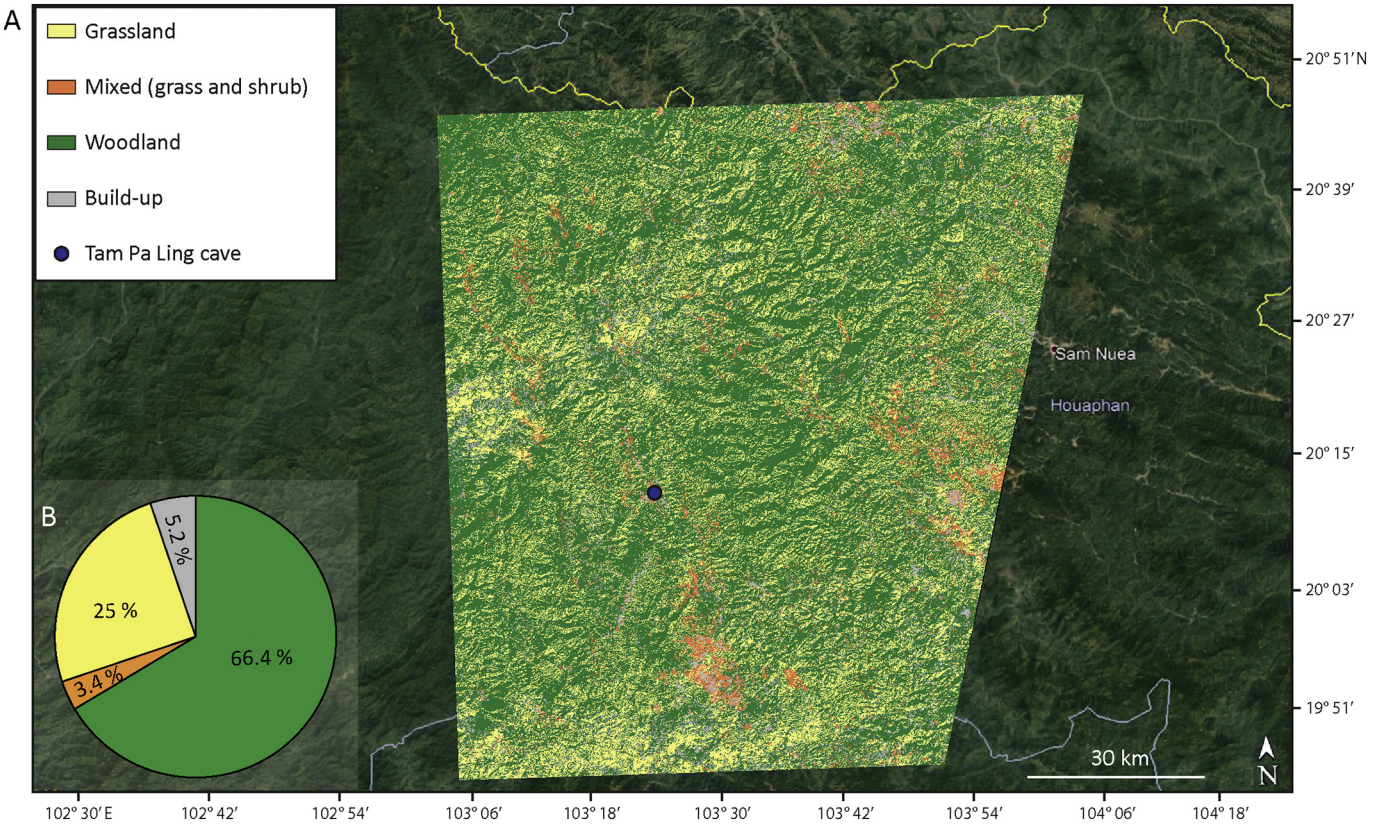

Fig. 3. (A) Land cover map obtained by analyzing Sentinel-2A satellite images using the software IMPACT Toolbox. The map shows the modern vegetation distribution around Tam Pà Ling cave. (B) Proportion of the single vegetation classes based on multi-band raster images. The graph is color-coded following the legend in the map. According to vegetation photosynthetic pathways, grassland and shrub (in yellow and orange) fall in the category of C_3 plants whereas woodland areas (in green) are dominated by C_4 plants. Build-up refers to the surface occupied by artificial infrastructures. (For interpretation of the references to color in this figure legend, the reader is referred to the web version of this article.)

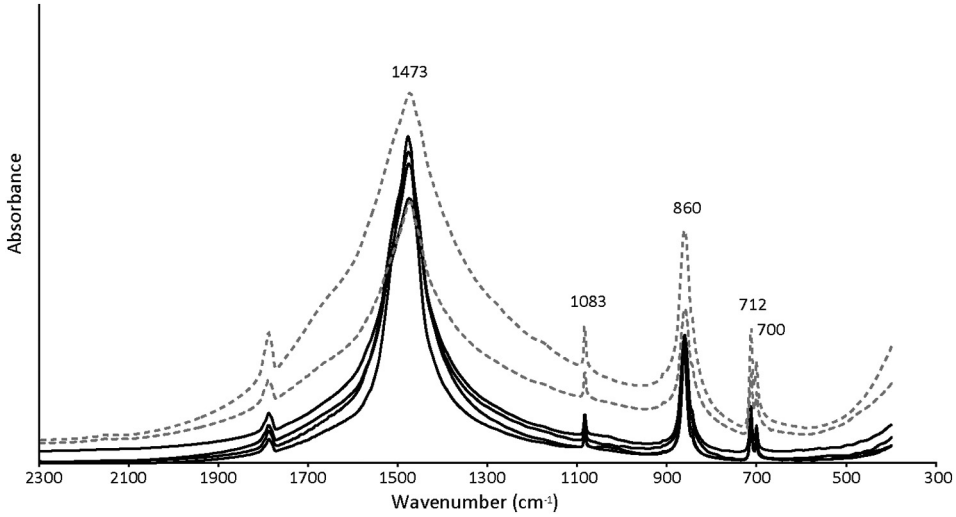

Fig. 4. FTIR spectra of modern (dashed lines) and archaeological (black lines) specimens of *Camaena massiei* showing the typical peaks of aragonite.

the shell carbon composition, the following mass balance equation was used:

$$\delta^{13}C_{shell} = \frac{(\delta^{13}C_{shell\ from\ C3\ plant} \times \%C_{consumed\ C3\ plant}) + (\delta^{13}C_{shell\ from\ C4\ plant} \times \%C_{consumed\ C4\ plant})}{(\%C_{consumed\ C3\ plant}) + (\%C_{consumed\ C4\ plant})}$$

The predicted shell $\delta^{13}C$ values obtained were then compared to the carbon isotope composition of the modern specimens in relation to the C_3 and C_4 distribution measured by remote sensing.

4. Results

4.1. Modern environmental context

The annual precipitation in the area is 1902.7 mm, with a minimum during the dry season of 50.5 mm (November–April) and a maximum during the wet season (May–October) of 266.7 mm. The relative humidity ranges between 77.6% (dry season) and 83.4% (wet season), with an annual average of 80.5% (Fig. 2A). The average annual temperature is 21.5 °C, ranging from 15.7 °C in December to 25.3 °C in June and July. Rainfall $\delta^{18}O$ varies between −10.6‰ in August and −4.5‰ in April, with an annual average of −7.3‰ (Fig. 2B). Because land snails in tropical and subtropical environments tend to grow their shells all year round (Yanes and Fernández-Lopez-de-Pablo, 2017), shell stable isotope data were compared to the monthly instrumental data covering the full year.

Remote sensing data indicate that the primary land cover component around TPL consists of woody plants (C_3) contributing 66.4% to the overall vegetation, whereas grasslands and shrubs (C_4) occupy 28.4% of the analyzed surface. Areas dedicated to build up account for 5.2% (Fig. 3). When taking into account only the surface occupied by natural vegetation, discarding the areas occupied by artificial infrastructures, the contributions of C_3 and C_4 plants account for 70.1% and 26.3%, respectively.

4.2. Shell mineralogy and stable isotope composition

As shown by the two modern specimens analyzed using FTIR (TPL_M1 and TPL_M2), *C. massiei* shell is completely aragonitic. Their spectra display the five typical aragonite peaks related to carbonate ion vibrational modes: the ν_3 asymmetric stretch at 1473 cm^{-1}, the ν_1 symmetric stretch at 1083 cm^{-1}, the ν_2 out-of-plane bending at 860 cm^{-1} and the ν_4 C–O in-plane bending doublet at 712 and 700 cm^{-1} (Fig. 4). Likewise, the archaeological specimens present the same spectra as the modern shells, excluding the possibility of diagenetic alteration and validating the suitability of using these materials for geochemical analyses (Fig. 4).

Details on the individual oxygen and carbon isotope values are found in Supplementary information (SI 1). Modern *C. massiei* shells are characterized by an average $\delta^{13}C$ of −8.7‰ ± 1.7 and $\delta^{18}O$ of −7.6‰ ± 1.7 (Fig. 5B–C). The average shell $\delta^{18}O$ is slightly more positive than the annual recorded rainfall $\delta^{18}O$ in the area by +0.4‰. Based on the two-source input mass balance model, the $\delta^{13}C$ values relate to a diet mainly composed by C_3 vegetation (76%) with a minor contribution of C_4 plants (24%; Fig. 6).

The $\delta^{13}C$ of archaeological shells ranges between −12.1‰ and −1.8‰ with an average of −7.7 ± 2.6‰ (n = 49). The $\delta^{18}O$ of archaeological shells varies between −11.6‰ and −5.5‰ with an average of −7.8 ± 1.5‰ (Fig. 5A). The scatter of the isotope data appears broader in age groups containing larger number of specimens suggesting that it may be related to a certain degree of inter-individual variability. The oldest age group (62–78 ka) contains only one specimen with $\delta^{13}C$ of −8.6‰ and $\delta^{18}O$ of −7.2‰ (Fig. 5B–C). The reconstructed diet comprehends 75% of C_3 vegetation and 25% of C_4 vegetation (Fig. 6). The age groups from 62 ka to 32 ka (n = 30) are formed by shells with similar isotopic compositions, with an average $\delta^{13}C$ of −8.9 ± 2.9‰ and an average $\delta^{18}O$ value of −8.1 ± 1.4‰ (Fig. 5B–C). According to these $\delta^{13}C$ values, C_3 plants are estimated to contribute from 73% to 82% of the snail diet (Fig. 6). The shells dated 21–25 ka (n = 4) are characterized by higher values, with an average $\delta^{13}C$ of −4.0 ± 2.4‰ and $\delta^{18}O$ of −6.3 ± 0.8‰ (Fig. 5B–C). In these specimens, C_3 plants are suggested to contribute only to 32% of snail diet whereas C_4 vegetation contributes to 68% (Fig. 6). Similarly, the shells from the 12–16 ka age group (n = 5) show relative positive isotopic profiles with $\delta^{13}C$ of −5.1 ± 1.7‰ and $\delta^{18}O$ of −6.7 ± 1.2‰ (Fig. 5B–C). In these cases, the diet is composed by 42% of C_3 and 58% of C_4 plants (Fig. 6). To the youngest cluster (0.9 ± 3 ka) belong shells (n = 9) with average $\delta^{13}C$ of −7.4‰ ± 1.7 and $\delta^{18}O$ of −8.7‰ ± 1.7 (Fig. 5B–C). In this case, C_3 plants account for 64% of the diet and C_4 account for 36% (Fig. 6).

5. Discussion

5.1. Shell oxygen isotope record and rainfall variability

The oxygen isotope composition of the modern *C. massiei* shells shows a slight enrichment in ^{18}O compared to the rainfall in the area. This offset is known to be related to fractionation associated with

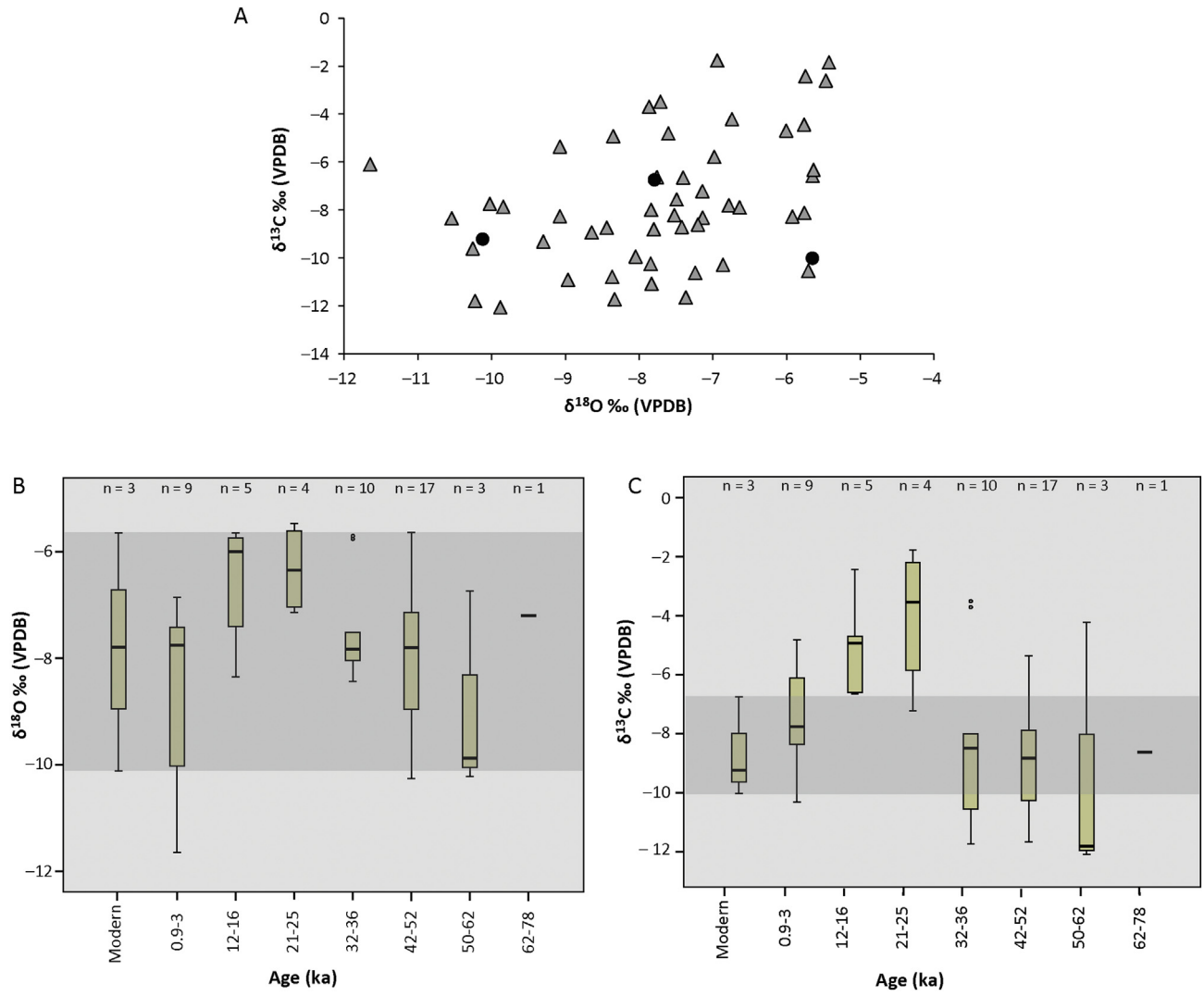

Fig. 5. Isotopic composition of *Camaena massiei* shells. (A) Scatterplot of carbon and oxygen stable isotopes. Grey triangles represent archaeological shells and black circle modern specimens. (B–C) Boxplots of $\delta^{13}C$ and $\delta^{18}O$ of modern and archaeological shells divided in age groups according to their position in the stratigraphic sequence. The highlighted areas indicate the modern isotopic range. Dots in the graphs represent outliers.

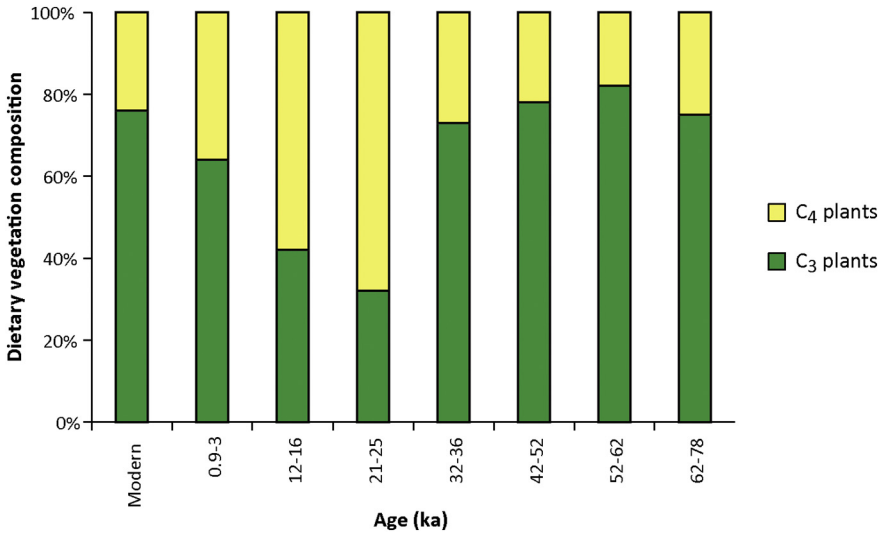

Fig. 6. Vegetation composition as C_3 and C_4 plant proportions derived from shell $\delta^{13}C$ values.

evaporation and animal physiological processes (Yapp, 1979; Balakrishnan and Yapp, 2004). For instance, the ^{18}O enrichment in snail fluids and therefore in the shell composition is controlled by the combination of several factors such as air temperature, relative humidity, water vapor $\delta^{18}O$ and $\delta^{18}O$ composition of the ingested liquid water (Balakrishnan and Yapp, 2004).

Our results indicate a certain degree of variability in shell $\delta^{18}O$ through time, which is likely related to changes in amount of precipitation during the Late Pleistocene and the Holocene. To strengthen the interpretation of the associated climatic patterns, these data are compared to the existing terrestrial $\delta^{18}O$ records in the region. Among the data are Hulu cave stalagmites from Jiangsu province, east China (from 75 to 11 ka) and the speleothem from Dongge cave from Guizhou province, southwest China (from 16 ka to modern times). As in shell carbonate, speleothem $\delta^{18}O$ variability is influenced by changes in the amount of precipitation affecting the isotopic signature of the meteoric water. For instance, low stalagmite $\delta^{18}O$ values correspond to low $\delta^{18}O$ rainfall, which is the result of an increase in the amount of precipitation (Wang, 2001; Yuan et al., 2004). Since in Laos the rainfall is primarily controlled by the summer monsoon transporting moisture and heat from Australia northward (Ribolzi et al., 2008), the $\delta^{18}O$ variability recorded in terrestrial paleoarchives can be also used as proxy for reconstructing past monsoon intensity (Wang, 2001).

The $\delta^{18}O$ profiles of the archaeological shells from Tam Pà Ling present an analogous trend to the Chinese speleothem data (Fig. 7). Besides its environmental significance, the temporal correspondence between the two datasets further corroborates the chronological sequence at Tam Pà Ling. By strengthening the robustness of the dating, shell $\delta^{18}O$ profiles contribute to an improvement in the contextualization of the modern human remains. From the environmental perspective, only one *C. massiei* specimen was retrieved from sediments dated to 70 ± 8 ka, therefore the interpretation of local conditions during this time has to be taken with caution. The shell indicates that in northeast Laos the rainfall during the MIS 5 and MIS 4 transition was less abundant than the late MIS 4 and MIS 3. Similarly, the magnetic susceptibility (at Tam Pà Ling) indicates a dry climate at the MIS 5-MIS 4 transition and a trend toward wetter conditions during early MIS 3. Subsequently, between 51.6 and 35 ka, a progressive aridity is recorded (Luu Thi Phuong Lan, unpublished data; see Supplementary information SI 2). Similar results were previously inferred from the Chinese loess plateau indicating weak summer monsoon intensity during MIS 5 (Chen et al., 1999).

During late MIS 4 and MIS 3 northeast Laos is suggested to be characterized by a wet climate. During these time periods, Tam Pà Ling pollen record contains evidence of taxa (i.e., *Pinus* sp., *Abies* sp. and *Myrica* sp.) typical of temperate and tropical mountainous habitats characterized by wet conditions (Nguyen Thi Mai Huongh, unpublished data). Similarly, the palynological record in the Yunnan province supported the evidence of humid conditions before the LGM (Walker, 1986). Comparable climatic circumstances were inferred in the lower Mun River Basin, northeast Thailand, where geomorphological features showed accumulation of organic matter between 20 and 40 ka (Löffler et al., 1984). Furthermore, the $\delta^{18}O$ composition of the freshwater bivalve *Margaritanopsis laoensis* indicated elevated rainfall during MIS 3 (Marwick and Gagan, 2011). Likewise the shells analyzed in this study, the stalagmites from Hulu cave presented a gradual trend toward higher values from late MIS 3 to early MIS 2 (Wang, 2001; Fig. 7). However, it is relevant to note that *C. massiei* shells record slightly more arid conditions compared to the speleothems during the late phases of MIS 3 implying that part of the climatic signal is not stored in shell data. The interpretation of such offset may not be straightforward and additional material would be needed to gain a deeper understanding of the dynamics occurring during this period. Nevertheless, these observations contribute to an overall picture of a wet Late Pleistocene presumably related to strong monsoon intensity.

After this wet phase, a sharp increase in shell $\delta^{18}O$ occurred between 25 and 12 ka. This coincided with a change toward higher values in Hulu and Dongge caves speleothems occurring until ~11 ka (Wang, 2001; Yuan et al., 2004; Fig. 7). All records suggest a decrease in the amount of rainfall indicating a dry period during MIS 2. This is also supported by the magnetic susceptibility data that show a general decrease in humidity between 29.8 and 3 ka (Luu Thi Phuong Lan, unpublished data; see SI 2).

Significant aridity during this phase has been previously recorded in the form of vegetation shift and loess formation (Penny, 2001). Such extreme aridity is potentially related to the decrease in the sea level during LGM and to changes in the atmosphere-ocean circulation patterns. The expansion of the exposed continental shelves during the LGM may have decreased the water evaporation from the ocean and diminished the moisture carried by monsoon winds with a substantial

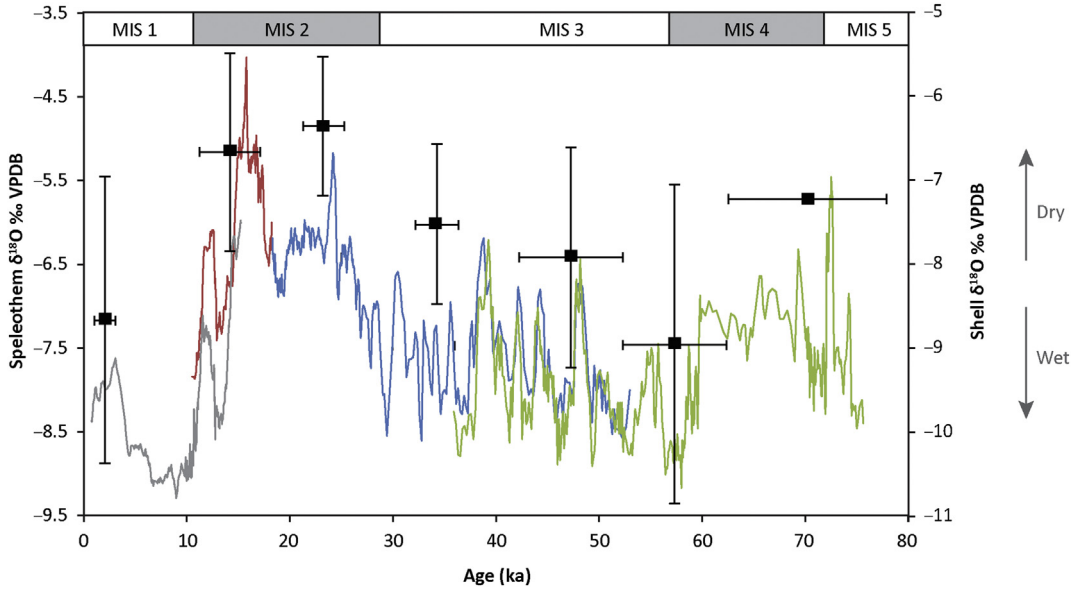

Fig. 7. Comparison between shell oxygen isotope composition (black squares and secondary y-axis) and stalagmites from Dongge cave (grey line) and Hulu cave (red line: PD speleothem; blue line: MSD speleothem; green line: MSL speleothem). (For interpretation of the references to color in this figure legend, the reader is referred to the web version of this article.)

decline in rainfall over Laos and the rest of Indochina (Heaney, 1991). Furthermore, a southward shift of the intertropical convergence zone and the reduced difference in heat distribution between ocean and land masses weakened the Walker circulation and it contributed to a sharp decrease in the summer monsoon strength (Stott et al., 2002).

During the Holocene, around 2 ± 1 ka *C. massiei* shells show $\delta^{18}O$ values decreasing again toward more negative values. The speleothem from Dongge cave also presented lower values during the Holocene compared to the MIS 2 Hulu cave record. It must be noted that the small offset between the two caves visible in Fig. 7 can be explained by the so called "Altitude Effect". Dongge cave stalagmites, being located at higher altitude (680 m a.s.l.), are expected to have more negative $\delta^{18}O$ values than Hulu cave (100 m a.s.l.) due to the fact that rainwater becomes isotopically lighter with altitude because of Rayleigh distillation processes (Gonfiantini et al., 2001). Based on the difference in altitude between the two caves (ca. 580 m), the $\delta^{18}O$ rainfall altitude effect ranges between −1.0‰ and −1.3‰ (Peng et al., 2010). Aside from this, the Dongge cave stalagmite indicated that the Holocene was generally characterized by a warm and wet climate (Dykoski et al., 2005). Especially high monsoon intensity was recorded until ca 3.6 ka, when an increase in $\delta^{18}O$ indicated a shift toward drier conditions. Such change was indirectly related to a variation in the Earth's orbit that increased the summer insolation in the Northern Hemisphere and affected the temperature difference between land and ocean leading to a weakening of the monsoon winds (Dykoski et al., 2005). Due to a lack of shell material from the Early Holocene, this drying trend is not visible in the Tam Pà Ling record. However, our results show that the Late Holocene in northeast Laos has a comparable climate to that of the Late Pleistocene in terms of precipitation and monsoon intensity. In agreement with our results, pollen remains from Tam Pà Ling show the reappearance of coniferous vegetation (Nguyen Thi Mai Huongh, unpublished data).

5.2. Shell carbon isotope record and vegetation patterns

In modern shells, the calculated proportions of ingested C_3 (76%) and C_4 plants (24%) agree well with the vegetation coverage observations by remote sensing (Fig. 6). Satellite data illustrate a local environmental complexity with closed C_3-dominated rainforests representing the major vegetation component (70.1%), regularly interspersed with open woodlands and savanna habitats (26.3%). These data suggest that *C. massiei* is a generalist feeder, making use of the local available variety of the plant resources. Furthermore, the good agreement between the predicted vegetation distribution derived by the shell $\delta^{13}C$ signature and the observed vegetation patterns indicate that *C. massiei* do not ingest significant amount of foreign carbonates from the sediment. If that was the case, the shells would result enriched in ^{13}C and their $\delta^{13}C$ would be characterized by more positive values leading to an overestimation of the C_4 plants contribution to their diet. Such offset does not occur in the modern *C. massiei* and therefore any significant contribution by foreign carbonates to the shell composition can be discarded. Besides a minor overestimation in C_3 abundance, *C. massiei* shell geochemical profile is easily comparable with the expected values, suggesting $\delta^{13}C$ as an adequate paleovegetation proxy for the area of interest.

In archaeological Tam Pà Ling shells, the $\delta^{13}C$ profiles show a trend that closely follows the one observed for the $\delta^{18}O$ values (Fig. 5). During the Pleistocene until 32 ka, shell carbon isotope composition is especially depleted, indicating that the snail's diet major component consisted of C_3 plants. Data suggest that in this period the area surrounding Tam Pà Ling was characterized by similar habitats as compared to modern times, with slightly more abundant arboreal C_3 vegetation. Similarly, the preliminary data of the microvertebrate remains from Tam Pà Ling suggest the occurrence of local environmental changes. The record is dominated by two forest-dwelling rodent taxa (*Niviventer* sp., *Leopoldamys sabanus*) throughout the sequence (66% of all identified remains in the 2010–2015 record), indicating the persistence of a forested environment since ~70 ka. However, the record of rodent sub-family Arvicolinae seems to be more informative on climate changes. At present, the arvicolins are not found in Laos, but they are common at higher latitudes in Asia. Their presence is generally related to temperate habitats, with relatively cool temperatures (Corbet and Hill, 1992). Three distinct taxa are present at Tam Pà Ling. The first occurrence of an arvicolin taxon is during the age range ~42–52 ka, during the first half of MIS 3. This occurrence could correspond to a signal of a more arid climate. The group became more diversified with two more taxa in the age range ~21–36 ka, a period marked by the decline in temperatures of the LGM (26.5–19 ka; Clark et al., 2009).

In good agreement with these results, non-arboreal pollen is rather scarce in sediments from MIS 5, MIS 4 and the first half of MIS 3 (Nguyen Thi Mai Huongh, unpublished data). Recent zooarchaeological and isotopic evidences from Duoi U'Oi and Ma U'Oi in northern Vietnam (~200 km from Tam Pà Ling) indicated that during MIS 4 the area was characterized by mixed and open woodlands (Bacon et al., 2006; Bacon et al., 2018). All the results agree on the importance of the arboreal component. However, the diversity in altitude between the Vietnamese sites (~110 m) and Tam Pà Ling (1170 m) likely affected the tree biomass inducing denser forests to occur at higher elevations, as in modern times.

Several works have suggested that a significant aridity during MIS 2, and in particular during the LGM may have occurred inducing a substantial change in the vegetation. For instance, Zheng and Lei (1999) reported that between 29 and 15 ka in southern China (Leizhou Peninsula) the existing mixed forests were replaced by savannah-like environments in response to the temperature and rainfall drop. The same trend was observed in pollen records from ten different localities in Indochina and Southeast Asia (Kershaw et al., 2001). Furthermore, the scarce proportion of arboreal pollen relative to grasses, together with the evidence of frequent burnings in northeast Thailand indicated a pronounced dry climate during LGM (Kealhofer and Penny, 1998; Penny, 2001). Based on an exhaustive review of the existing sedimentological, zoological and fossil botanical data, Ray and Adams (2001) mapped the global vegetation distribution between 25 and 15 ka. Northern Laos was categorized as semi-arid temperate woodland or shrubs. The results of the current study agree well with these reconstructions, showing that the coverage of C_3 plants between 25 and 12 ka drastically decreased by ca 40% relative to previous Pleistocene times (Fig. 6). Likewise, a consistent increase in the occurrence of grass pollen (Poaceae) is noticeable in the palynological record of Tam Pà Ling from 33 ± 3 ka (Huong Mai, unpublished data). Although rarely, different scenarios implying less arid conditions were also suggested. For instance, the discovery of freshwater snails in LGM sediments (~18 ka) from Vietnam was interpreted by Viet (2008) as evidence for humid climatic conditions. Coastal site Hang Trống in norther Vietnam also displayed the persistence of tropical forests during the LGM (Rabett et al., 2017). However, such reconstructions were possibly geographically limited to the specific locations of the sites, in a valley and along the coast respectively.

After the LGM, pollen remains from northeast Thailand indicated a restoration and diversification of rich arboreal vegetation with increased precipitation (Kealhofer and Penny, 1998). Toward the end of the Holocene our shells indicate a similar vegetation composition than to present times, with a slightly reduced (ca −11%) C_3 plant coverage compared to the Late Pleistocene. This may be related to the tendency toward drier conditions occurring after the Holocene climatic optimum. Another hypothesis that has been proposed concerns the anthropogenic use of fire as a trigger for landscape change. Evidence of forest clearance was found in northeastern Thailand and this may have negatively affected the natural arboreal communities (Kealhofer and Penny, 1998; White et al., 2004). Similarly, the pollen record at Tam Pà Ling indicates that during this phase tropical and subtropical taxa and coniferous species are present, together with a larger representation of

grasses than Pleistocene times (Nguyen, unpublished data).

5.3. Environment and first Homo sapiens in Indochina

MIS 4 holds the first evidence of modern humans in Indochina (Demeter et al., 2017; Westaway et al., 2017). Our results indicate that during early MIS 4 monsoon intensity was potentially rather weak, with a significant strengthening during the late phase of MIS 4. Despite signs of reduced rainfall during early MIS 4, this did not translate to a major change of the landscape. In fact, arboreal vegetation was abundant in the area throughout the Late Pleistocene.

Based on the data presented here, the first *H. sapiens* to reach and become established in the area would have encountered wet and forested conditions. Generally, a wet climate is considered advantageous for human movements out of Africa and in areas otherwise dominated by deserts (Petraglia et al., 2010). However, in tropical and subtropical regions the interpretation may differ. In the case of Indochina, the rainforests occurring during MIS 4 supported the existence of a wide range of small to large terrestrial species. In particular, large ungulates were abundant in Duoi U'Oi, northern Vietnam (Bacon et al., 2018). Despite the high variety of potential game for humans, at present, the degree of exploitation of closed forests versus open landscapes is still an open question. Indications of technological development for hunting arboreal and semi-arboreal species are apparent in more recent contexts. For instance, numerous bone tools were recovered from Lobang Hangus, Niah Caves dating to the Terminal Pleistocene (Piper and Rabett, 2009). However, no artefacts have been found in older sites (MIS 4).

Even if very sparse, there are documented cases of early human occupation in the region that are coeval with Tam Pà Ling. Sites were found in northwest Laos, Cambodia and Thailand and they can help to interpret behaviors of the first modern humans in the region (White et al., 2004; Mudar and Anderson, 2007; Sophady et al., 2016). For instance, the analysis of the faunal assemblage at Lang Rongrien, in southern Thailand suggested that early populations (43–27 ka) were mostly hunting their game in open forests and grassland environments (Mudar and Anderson, 2007). This preference may suggest that before the development of specific tools, the main hunting activities were carried out in patches of low-density forests. Further examination of the Tam Pà Ling faunal assemblage associated with the *H. sapiens* remains will likely increase our understanding of the relationship between humans and the surrounding environment.

6. Conclusions

Analysis of modern specimens indicates that *C. massiei* shell carbon isotopes are suitable for paleoenvironmental reconstructions. The proportions of C_3 and C_4 vegetation inferred from modern land snail $\delta^{13}C$ closely reflect the distribution observed by remote satellite data, supporting the use of this proxy in future archaeological studies. Oxygen and carbon stable isotope signatures of Tam Pà Ling archaeological shells indicate that the earliest modern humans in the region experienced a humid climate together with woodland-dominated landscapes. These conditions drastically changed during the Last Glacial Maximum, when precipitation and monsoon strength decreased leading to the reduction of arboreal vegetation and favoring the expansion of more open environments. In addition, shell oxygen isotope profiles further confirm the dates at Tam Pà Ling, adding strength to the temporal contextualization of the first modern human remains in the region. Our results suggest that snail carbonates are suitable tools to complement the scattered terrestrial paleorecord in Southeast Asia.

Acknowledgments

The authors acknowledge the Authorities of the Department of National Heritage, Ministry of Information and Culture in Vientiane, Laos, for their authorization to work at Tam Pa Ling since 2009. This research was supported by the French Ministry of Foreign Affairs, the Ministry of Information, Culture and Tourism of Lao PDR, the University of Illinois at Urbana-Champaign, USA, the UPR2147 (CNRS, Paris), UMR7206 (MNHN, Paris), UMR5288 (AMIS), the UMR7516 (University of Strasbourg) and the Department of Human Evolution (Max Planck Institute for Evolutionary Anthropology, Leipzig). The authors thank Frank Sénégas (CR2P, UMR 7207, Sorbonne Universités - MNHN - CNRS – UMPC) for his contribution in the analysis of the microvertebrate remains from Tam Pà Ling and Dr. Barna Páll-Gergely for sharing his expertise on *C. massiei* taxonomy and ecology. The authors thank Dr. Paul Butler and two anonymous reviewers for providing constructive comments in the reviewing process.

Appendix A. Supplementary data

Supplementary data to this article can be found online at https://doi.org/10.1016/j.palaeo.2018.08.020.

References

Antoine, P., Limondin-Lozouet, N., 2004. Identification of MIS 11 interglacial tufa deposit in the Somme valley (France): new results from the Saint-Acheul fluvial sequence. Quaternaire 15, 41–52. https://doi.org/10.3406/quate.2004.1753.

Araguás-Araguás, L., Froehlich, K., Rozanski, K., 1998. Stable isotope composition of precipitation over southeast Asia. J. Geophys. Res. 103, 28721. https://doi.org/10.1029/98JD02582.

Bacon, A.M., Demeter, F., Roussé, S., Long, V.T., Duringer, P., Antoine, P.O., Thuy, N.K., Mai, B.T., Huong, N.T.M., Dodo, Y., Matsumura, H., Schuster, M., Anezaki, T., 2006. New palaeontological assemblage, sedimentological and chronological data from the Pleistocene Ma U'Oi cave (northern Vietnam). Palaeogeogr. Palaeoclimatol. Palaeoecol. 230, 280–298. https://doi.org/10.1016/j.palaeo.2005.07.023.

Bacon, A.M., Demeter, F., Tougard, C., de Vos, J., Sayavongkhamdy, T., Antoine, P.O., Bouasisengpaseuth, B., Sichanthongtip, P., 2008. Redécouverte d'une faune pléistocène dans les remplissages karstiques de Tam Hang au Laos: Premiers résultats. C.R. Palevol 7, 277–288. https://doi.org/10.1016/j.crpv.2008.03.009.

Bacon, A.M., Duringer, P., Antoine, P.O., Demeter, F., Shackelford, L., Sayavongkhamdy, T., Sichanthongtip, P., Khamdalavong, P., Nokhamaomphu, S., Sysuphanh, V., Patole-Edoumba, E., Chabaux, F., Pelt, E., 2011. The Middle Pleistocene mammalian fauna from Tam Hang karstic deposit, northern Laos: new data and evolutionary hypothesis. Quat. Int. 245, 315–332. https://doi.org/10.1016/j.quaint.2010.11.024.

Bacon, A.M., Bourgon, N., Dufour, E., Zanolli, C., Duringer, P., Ponche, J.L., Antoine, P.O., Shackelford, L., Huong, N.T.M., Sayavonkhamdy, T., Patole-Edoumba, E., Demeter, F., 2018. Nam Lot (MIS 5) and Duoi U'Oi (MIS 4) Southeast Asian sites revisited: zooarchaeological and isotopic evidences. Palaeogeogr. Palaeoclimatol. Palaeoecol. 1–13. https://doi.org/10.1016/j.palaeo.2018.03.034.

Badoux, D.M., 1959. Fossil Mammals From Two Deposits at Punung (Java). Kemink en Zoon, N.V., Utrecht.

Balakrishnan, M., Yapp, C.J., 2004. Flux balance models for the oxygen and carbon isotope compositions of land snail shells. Geochim. Cosmochim. Acta 68, 2007–2024. https://doi.org/10.1016/j.gca.2003.10.027.

Balakrishnan, M., Yapp, C.J., Meltzer, D.J., Theler, J.L., 2005. Paleoenvironment of the Folsom archaeological site, New Mexico, USA, approximately 10,500 14C yr B.P. as inferred from the stable isotope composition of fossil land snail shells. Quat. Res. 63, 31–44. https://doi.org/10.1016/j.yqres.2004.09.010.

Blinkhorn, J., Achyuthan, H., Petraglia, M., Ditchfield, P., 2013. Middle palaeolithic occupation in the Thar desert during the Upper Pleistocene: the signature of a modern human exit out of Africa? Quat. Sci. Rev. 77, 233–238. https://doi.org/10.1016/j.quascirev.2013.06.012.

Boivin, N., Fuller, D.Q., Dennell, R., Allaby, R., Petraglia, M.D., 2013. Human dispersal across diverse environments of Asia during the Upper Pleistocene. Quat. Int. 300, 32–47. https://doi.org/10.1016/j.quaint.2013.01.008.

Bonadonna, F., Leone, G., 1995. Palaeoclimatological reconstruction using stable isotope data on continental molluscs from Valle di Castiglione, Roma, Italy. The Holocene 5, 461–469. https://doi.org/10.1177/095968369500500409.

Bonadonna, F.P., Leone, G., Zanchetta, G., 1999. Stable isotope analyses on the last 30 ka molluscan fauna from Pampa grassland, Bonaerense region, Argentina. Palaeogeogr. Palaeoclimatol. Palaeoecol. 153, 289–308. https://doi.org/10.1016/S0031-0182(99)00063-2.

Bond, W.J., 2008. What limits trees in C_4 grasslands and savannas? Annu. Rev. Ecol. Evol. Syst. 39, 641–659. https://doi.org/10.1146/annurev.ecolsys.39.110707.173411.

Bowen, G.J., Wilkinson, B., 2002. Spatial distribution of $\delta^{18}O$ in meteoric precipitation. Geol. Soc. Am. Bull. 30, 315–318. https://doi.org/10.1130/0091-7613(2002)030<0315.

Bulbeck, D., 2007. Where river meets sea: a parsimonious model for *Homo sapiens* colonization of the Indian Ocean rim and Sahul. Curr. Anthropol. 48, 315–321.

Butler, P.G., Wanamaker, A.D., Scourse, J.D., Richardson, C.A., Reynolds, D.J., 2013. Variability of marine climate on the North Icelandic Shelf in a 1357-year proxy archive based on growth increments in the bivalve *Arctica islandica*. Palaeogeogr.

Palaeoclimatol. Palaeoecol. 373, 141–151. https://doi.org/10.1016/j.palaeo.2012.01.016.
Chen, F.H., Bloemendal, J., Feng, Z.D., Wang, J.M., Parker, E., Gou, Z.T., 1999. East Asian monsoon variations during Oxygen Isotope Stage 5: evidence from the northwestern margin of the Chinese loess plateau. Quat. Sci. Rev. 18, 1127–1135. https://doi.org/10.1016/S0277-3791(98)00047-X.
Chiba, S., Davison, A., 2009. Associations between stable carbon isotope ratio and vegetation in modern and fossil land snails *Mandarina chichijimana* on Chichijima of the Ogasawara Islands. Paleontol. Res. 13, 151–157. https://doi.org/10.2517/1342-8144-13.2.151.
Clark, P.U., Dyke, A.S., Shakun, J.D., Carlson, A.E., Clark, J., Wohlfarth, B., Mitrovica, J.X., Hostetler, S.W., McCabe, A.M., 2009. The Last Glacial Maximum. Science 325, 710–714. https://doi.org/10.1126/science.1172873.
Colonese, A.C., Zanchetta, G., Dotsika, E., Drysdale, R.N., Fallick, A.E., Grifoni Cremonesi, R., Manganelli, G., 2010. Early-middle Holocene land snail shell stable isotope record from Grotta di Latronico 3 (southern Italy). J. Quat. Sci. 25, 1347–1359. https://doi.org/10.1002/jqs.1429.
Corbet, G.B., Hill, J.E. (Eds.), 1992. The Mammals of the Indomalayan Region: A Systematic Review. Oxford University Press, New York.
Dansgaard, W., 1964. Stable isotopes in precipitation. Tellus 16, 436–468. https://doi.org/10.3402/tellusa.v16i4.8993.
Demeter, F., Sayavongkhamdy, T., Patole-Edoumba, E., Coupey, A.-S., Bacon, A.-M., De Vos, J., Tougard, C., Bouasisengpaseuth, B., Sichanthongtip, P., Duringer, P., 2009. Tam Hang Rockshelter: preliminary study of a prehistoric site in northern Laos. Asian Perspect. 48, 291–308. https://doi.org/10.1353/asi.2009.0000.
Demeter, F., Shackelford, L.L., Bacon, A.-M., Duringer, P., Westaway, K., Sayavongkhamdy, T., Braga, J., Sichanthongtip, P., Khamdalavong, P., Ponche, J.-L., Wang, H., Lundstrom, C., Patole-Edoumba, E., Karpoff, A.-M., 2012. Anatomically modern human in Southeast Asia (Laos) by 46 ka. Proc. Natl. Acad. Sci. 109, 14375–14380. https://doi.org/10.1073/pnas.1208104109.
Demeter, F., Shackelford, L., Westaway, K., Duringer, P., Bacon, A.M., Ponche, J.L., Wu, X., Sayavongkhamdy, T., Zhao, J.X., Barnes, L., Boyon, M., Sichanthongtip, P., Sénégas, F., Karpoff, A.M., Patole-Edoumba, E., Coppens, Y., Braga, J., 2015. Early modern humans and morphological variation in Southeast Asia: fossil evidence from Tam Pà Ling, Laos. PLoS One 10, 1–17. https://doi.org/10.1371/journal.pone.0121193.
Demeter, F., Shackelford, L., Westaway, K., Barnes, L., Duringer, P., Ponche, J.-L., Dumoncel, J., Sénégas, F., Sayavongkhamdy, T., Zhao, J.-X., Sichanthongtip, P., Patole-Edoumba, E., Dunn, T., Zachwieja, A., Coppens, Y., Willerslev, E., Bacon, A.-M., 2017. Early modern humans from Tam Pà Ling, Laos: fossil review and perspectives. Curr. Anthropol. 58, S527–S538. https://doi.org/10.1086/694192.
Duringer, P., Bacon, A.M., Sayavongkhamdy, T., Nguyen, T.K.T., 2012. Karst development, breccias history, and mammalian assemblages in Southeast Asia: a brief review. C.R. Palevol 11, 133–157. https://doi.org/10.1016/j.crpv.2011.07.003.
Dykoski, C.A., Edwards, R.L., Cheng, H., Yuan, D., Cai, Y., Zhang, M., Lin, Y., Qing, J., An, Z., Revenaugh, J., 2005. A high-resolution, absolute-dated Holocene and deglacial Asian monsoon record from Dongge Cave, China. Earth Planet. Sci. Lett. 233, 71–86. https://doi.org/10.1016/j.epsl.2005.01.036.
Fromaget, J., 1936. Sur la stratigraphie des formations récentes de la Chaîne annamitique septentrionale et sur l'existence de l'Homme dans le Quaternaire inférieur de cette partie de l'Indochine. C. R. Acad. Sci. Paris 203, 738–741.
Fromaget, J., 1937. Aperçu sur la Stratigraphie et l'Anthropologie préhistorique des formations récentesdans la Chaîne Annamitique et le Haut-Laos. Compte rendu de la douzième session du Congrès préhistorique de France, Toulouse-Foix. pp. 785–798.
Fromaget, J., 1940. Les récentes découvertes anthropologiques dans les formations préhistoriques de la chaîne annamitique. Government Printer, Singapore, pp. 51–59.
Gonfiantini, R., Roche, M., Olivry, J., Fontes, J.-C., Zuppi, G.M., 2001. The altitude effect on the isotopic composition of tropical rains. Chem. Geol. 181, 147–167. https://doi.org/10.1016/S0009-2541(01)00279-0.
Goodfriend, G.A., 1988. Mid-Holocene rainfall in the Negev Desert from 13C of land snail shell organic matter. Nature 333, 757–760. https://doi.org/10.1038/333757a0.
Goodfriend, G.A., 1999. Terrestrial stable isotope records of late Quaternary paleoclimates in the eastern Mediterranean region. Quat. Sci. Rev. 18, 501–513. https://doi.org/10.1016/S0277-3791(98)00092-4.
Goodfriend, G.A., Ellis, G.L., 2002. Stable carbon and oxygen isotopic variations in modern *Rabdotus* land snail shells in the southern Great Plains, USA, and their relation to environment. Geochim. Cosmochim. Acta 66, 1987–2002. https://doi.org/10.1016/s0016-7037(02)00824-4.
Goodfriend, G.A., Stipp, J.J., 1983. Limestone and the problem of radiocarbon dating of land snail shell carbonate. Geology 11, 575–577. https://doi.org/10.1130/0091-7613(1983)11<575:latpor>2.0.co;2.
Gupta, A., 2009. Geology and landforms of the Mekong Basin. In: The Mekong, pp. 29–51. https://doi.org/10.1016/B978-0-12-374026-7.00003-6.
Heaney, L.R., 1991. A synopsis of climatic and vegetational change in Southeast Asia. Clim. Chang. 19, 53–61. https://doi.org/10.1007/BF00142213.
Hershkovitz, I., Weber, G.W., Quam, R., Duval, M., Grün, R., Kinsley, L., Ayalon, A., Bar-matthews, M., Valladas, H., Mercier, N., Arsuaga, J.L., Martinon-Torres, M., Bermudez de Castro, J.M., Fornai, C., Martin-Frances, L., Sarig, R., May, H., Krenn, V.A., Slon, V., Rodriguez, L., Garcia, R., Lorenzo, C., Carretero, J.M., Frumkin, A., Shahack-Gross, R., Bar-Yosef Mayer, D.E., Cui, Y., Wu, X., Peled, N., Groman-Yaroslavski, I., Weissbrod, L., Yeshurun, R., Tsatskin, A., Zaidner, Y., Weinstein-Evron, M., 2018. The earliest modern humans outside Africa. Science 359, 456–459.
Jones, D.S., 1983. Sclerochronology: reading the record of the molluscan shell. Am. Sci. 71, 384–391.
Kealhofer, L., Penny, D., 1998. A combined pollen and phytolith record for fourteen thousand years of vegetation change in northeastern Thailand. Rev. Palaeobot. Palynol. 103, 83–93. https://doi.org/10.1016/S0034-6667(98)00029-3.
Kershaw, A.P., Penny, D., van der Kaars, S., Anshari, G., Thamotherampillai, A., 2001. Vegetation and climate in lowland southeast Asia at the Last Glacial Maximum. In: Faunal and Floral Migrations and Evolution in SE Asia–Australasia. Balkema, Lisse, pp. 227–236.
Kohn, M.J., 2010. Carbon isotope compositions of terrestrial C_3 plants as indicators of (paleo)ecology and (paleo)climate. Proc. Natl. Acad. Sci. 107, 19691–19695. https://doi.org/10.1073/pnas.1004933107.
Leng, M.J., Lewis, J.P., 2016. Oxygen isotopes in molluscan shell: applications in environmental archaeology. Environ. Archaeol. 21, 295–306. https://doi.org/10.1179/1749631414y.0000000048.
Leng, M.J., Heaton, T.H.E., Lamb, H.F., Naggs, F., 1998. Carbon and oxygen isotope variations within the shell of an African land snail (*Limicolaria kambeul chudeaui* Germain): a high-resolution record of climate seasonality? The Holocene 8, 407–412. https://doi.org/10.1191/095968398669296159.
Liu, W., Martinón-Torres, M., Cai, Y.J., Xing, S., Tong, H.W., Pei, S.W., Sier, M.J., Wu, X.H., Edwards, R.L., Cheng, H., Li, Y.Y., Yang, X.X., De Castro, J.M.B., Wu, X.J., 2015. The earliest unequivocally modern humans in southern China. Nature 526, 696–699. https://doi.org/10.1038/nature15696.
Löffler, E., Thompson, W.P., Liengsakul, M., 1984. Quaternary geomorphological development of the lower Mun River Basin, North East Thailand. Catena 11, 321–330. https://doi.org/10.1016/0341-8162(84)90030-4.
Marković, S.B., Oches, E., Sümegi, P., Jovanović, M., Gaudenyi, T., 2006. An introduction to the Middle and Upper Pleistocene loess-paleosol sequence at Ruma brickyard, Vojvodina, Serbia. Quat. Int. 149, 80–86. https://doi.org/10.1016/j.quaint.2005.11.020.
Marwick, B., Gagan, M.K., 2011. Late Pleistocene monsoon variability in northwest Thailand: an oxygen isotope sequence from the bivalve *Margaritanopsis laosensis* excavated in Mae Hong Son province. Quat. Sci. Rev. 30, 3088–3098. https://doi.org/10.1016/j.quascirev.2011.07.007.
Mercier, N., Valladas, H., Bar-Yosef, O., Vandermeersch, B., Stringer, C., Joron, J.L., 1993. Thermoluminescence date for the mousterian burial site of Es-Skhul, Mt. Carmel. J. Archaeol. Sci. https://doi.org/10.1006/jasc.1993.1012.
Metref, S., Rousseau, D.D., Bentaleb, I., Labonne, M., Vianey-Liaud, M., 2003. Study of the diet effect on δ13C of shell carbonate of the land snail *Helix aspersa* in experimental conditions. Earth Planet. Sci. Lett. 211, 381–393. https://doi.org/10.1016/S0012-821X(03)00224-3.
Michel, V., Valladas, H., Shen, G., Wang, W., Zhao, J. xin, Shen, C.C., Valensi, P., Bae, C.J., 2016. The earliest modern *Homo sapiens* in China. J. Hum. Evol. 101, 101–104. https://doi.org/10.1016/j.jhevol.2016.07.008.
Milano, S., Schöne, B.R., Witbaard, R., 2017. Changes of shell microstructural characteristics of *Cerastoderma edule* (Bivalvia) - a novel proxy for water temperature. Palaeogeogr. Palaeoclimatol. Palaeoecol. 465, 395–406. https://doi.org/10.1016/j.palaeo.2015.09.051.
Mudar, K., Anderson, D.D., 2007. New evidence for Southeast Asian Pleistocene Foraging Economies: faunal remains from the early levels of Lang Rongrien Rockshelter, Krabi, Thailand. Asian Perspect. 46, 298–334. https://doi.org/10.1353/asi.2007.0013.
Peng, T.R., Wang, C.H., Huang, C.C., Fei, L.Y., Chen, C.T.A., Hwong, J.L., 2010. Stable isotopic characteristic of Taiwan's precipitation: a case study of western Pacific monsoon region. Earth Planet. Sci. Lett. 289, 357–366. https://doi.org/10.1016/j.epsl.2009.11.024.
Penny, D., 2001. A 40,000 year palynological record from north-east Thailand; implications for biogeography and palaeo-environmental reconstruction. Palaeogeogr. Palaeoclimatol. Palaeoecol. 171, 97–128. https://doi.org/10.1016/S0031-0182(01)00242-5.
Petraglia, M.D., Haslam, M., Fuller, D.Q., Boivin, N., Clarkson, C., 2010. Out of Africa: new hypotheses and evidence for the dispersal of *Homo sapiens* along the Indian Ocean rim. Ann. Hum. Biol. 37, 288–311. https://doi.org/10.3109/03014461003639249.
Piper, P.J., Rabett, R.J., 2009. Hunting in a tropical rainforest: evidence from the terminal Pleistocene at Lobang Hangus, Niah Caves, Sarawak. Int. J. Osteoarchaeol. 19, 551–565. https://doi.org/10.1002/oa.
Prendergast, A.L., Stevens, R.E., O'Connell, T.C., Hill, E.A., Hunt, C.O., Barker, G.W., 2016. A late Pleistocene refugium in Mediterranean North Africa? Palaeoenvironmental reconstruction from stable isotope analyses of land snail shells (Haua Fteah, Libya). Quat. Sci. Rev. 139, 94–109. https://doi.org/10.1016/j.quascirev.2016.02.014.
Prior, D.J., 1985. Water-regulatory behaviour in terrestrial gastropods. Biol. Rev. 60, 403–424. https://doi.org/10.1111/j.1469-185X.1985.tb00423.x.
Rabett, R., Ludgate, N., Stimpson, C., Hill, E., Hunt, C., Ceron, J., Farr, L., Morley, M., Reynolds, T., Zukswert, H., Simpson, D., Nyiri, B., Verhoeven, M., Appleby, J., Meneely, J., Phan, L., Dong, N.N., Lloyd-Smith, L., Hawkes, J., Blyth, A., Tâń, N.C., 2017. Tropical limestone forest resilience and late Pleistocene foraging during MIS-2 in the Tràng An massif, Vietnam. Quat. Int. 448, 62–81. https://doi.org/10.1016/j.quaint.2016.06.010.
Ray, N., Adams, J.M., 2001. A GIS-based vegetation map of the world at the Last Glacial Maximum. Internet Archaeol. 11, 0–15.
Reynolds, D.J., Scourse, J.D., Halloran, P.R., Nederbragt, A.J., Wanamaker, A.D., Butler, P.G., Richardson, C.A., Heinemeier, J., Eiríksson, J., Knudsen, K.L., Hall, I.R., 2016. Annually resolved North Atlantic marine climate over the last millennium. Nat. Commun. 7, 13502.
Rhoads, D.C., Pannella, G., 1970. The use of molluscan shell growth patterns in ecology and paleoecology. Lethaia 3, 143–161. https://doi.org/10.1111/j.1502-3931.1970.tb01854.x.
Ribolzi, O., Cuny, J., Sengsoulichanh, P., Pierret, A., Thiebaux, J.P., Huon, S., Bourdon, E., Robain, H., Sengtaheuangoung, O., 2008. Assessment of water quality along a

tributary of the Mekong River in a mountainous, mixed land-use environment of the Lao PDR. Lao J. Agric. For. 7, 92–111.
Rousseau, D.D., 2001. Loess biostratigraphy: new advances and approaches in mollusk studies. Earth Sci. Rev. 54, 157–171. https://doi.org/10.1016/S0012-8252(01)00046-0.
Rozanski, K., Araguás-Araguás, L., Gonfiantini, R., 1993. Isotopic patterns in modern global precipitation. In: Union, A.G. (Ed.), Climate Change in Continental Isotopic Records. American Geophysical Union Geophysical Monograph, vol. 78. American, Washington, DC, pp. 1–36. https://doi.org/10.1029/GM078p0001.
Sage, R.F., 2004. The evolution of C_4 photosynthesis. New Phytol. 161, 341–370. https://doi.org/10.1046/j.1469-8137.2004.00974.x.
Sage, R.F., Wedin, D.A., Li, M., 1999. The biogeography of C_4 photosynthesis: patterns and controlling factors. In: C_4 Plant Biology, pp. 313–373.
Schöne, B.R., Pfeiffer, M., Pohlmann, T., Siegismund, F., 2005. A seasonally resolved bottom-water temperature record for the period AD 1866–2002 based on shells of *Arctica islandica* (Mollusca, North Sea). Int. J. Climatol. 25, 947–962. https://doi.org/10.1002/joc.1174.
Schwarcz, H.P., Grün, R., Vandermeersch, B., Bar-Yosef, O., Valladas, H., Tchernov, E., 1988. ESR dates for the hominid burial site of Qafzeh in Israel. J. Hum. Evol. 17, 733–737. https://doi.org/10.1016/0047-2484(88)90063-2.
Scott, B., 1996. Phylogenetic relationships of the Camaenidae (Pulmonata: Stylommatophora: Helicoidea). J. Molluscan Stud. 62, 65–73. https://doi.org/10.1093/mollus/62.1.65.
Shackelford, L., Demeter, F., Westaway, K., Duringer, P., Ponche, J.L., Sayavongkhamdy, T., Zhao, J.X., Barnes, L., Boyon, M., Sichanthongtip, P., Sénégas, F., Patole-Edoumba, E., Coppens, Y., Dumoncel, J., Bacon, A.M., 2018. Additional evidence for early modern human morphological diversity in Southeast Asia at Tam Pà Ling, Laos. Quat. Int. 466, 93–106. https://doi.org/10.1016/j.quaint.2016.12.002.
Simonetti, D., Marelli, A., Eva, H.D., 2015. IMPACT Toolbox, a Portable Open Source GIS Toolbox for Image Processing and Land Cover Mapping. Publications Office of the European Union978-92-79-50115-9https://doi.org/10.2788/143497.
Solem, A., Christensen, C.C., 1984. Camaenid land snail reproductive cycle and growth patterns in semiarid areas of North-Western Australia. Aust. J. Zool. 32, 471–491.
Sophady, H., Forestier, H., Zeitoun, V., Puaud, S., Frère, S., Celiberti, V., Westaway, K., Mourer, R., Mourer-Chauviré, C., Than, H., Billault, L., Tech, S., 2016. Laang Spean cave (Battambang province): a tale of occupation in Cambodia from the Late Upper Pleistocene to Holocene. Quat. Int. 416, 162–176. https://doi.org/10.1016/j.quaint.2015.07.049.
Storm, P., De Vos, J., 2006. Rediscovery of the late pleistocene punung hominin sites and the discovery of a new site Gunung Dawung in East Java. Senckenb. Lethaea 86, 271–281. https://doi.org/10.1007/BF03043494.
Storm, P., Aziz, F., de Vos, J., Kosasih, D., Baskoro, S., Ngaliman, van de Hoek Ostende, L.W., 2005. Late Pleistocene *Homo sapiens* in a tropical rainforest fauna in East Java. J. Hum. Evol. 49, 536–545. https://doi.org/10.1016/j.jhevol.2005.06.003.
Stott, L.D., 2002. The influence of diet on the $\delta^{13}C$ of shell carbon in the pulmonate snail *Helix aspersa*. Earth Planet. Sci. Lett. 195, 249–259. https://doi.org/10.1016/S0012-821X(01)00585-4.
Stott, L., Poulsen, C., Lund, S., Thunell, R., 2002. Super ENSO and global climate time oscillations at millennial scales. Science 297, 222–226. https://doi.org/10.1126/science.1071627.
Stringer, C., 2000. Coasting out of Africa. Nature 405, 24–27. https://doi.org/10.1038/35011166.
Viet, N., 2008. Hoabinhian macrobotanical remains from archaeological sites in Vietnam: indicators of climate changes from the late Pleistocene to the early Holocene. Indo-Pacific Prehistory Assoc. Bull. 28, 80–83.
Walker, D., 1986. Late Pleistocene-Early Holocene vegetational and climatic changes in Yunnan Province, Southwest China. J. Biogeogr. 13, 477–486.
Wang, Y.J., 2001. A high-resolution absolute-dated Late Pleistocene monsoon record from Hulu Cave, China. Science 294, 2345–2348. https://doi.org/10.1126/science.1064618.
Westaway, K.E., Morwood, M.J., Roberts, R.G., Rokus, A.D., Zhao, J.x., Storm, P., Aziz, F., van den Bergh, G., Hadi, P., Jatmiko, de Vos, J., 2007. Age and biostratigraphic significance of the Punung Rainforest Fauna, East Java, Indonesia, and implications for *Pongo* and *Homo*. J. Hum. Evol. 53, 709–717. https://doi.org/10.1016/j.jhevol.2007.06.002.
Westaway, K.E., Louys, J., Awe, R.D., Morwood, M.J., Price, G.J., Zhao, J.X., Aubert, M., Joannes-Boyau, R., Smith, T.M., Skinner, M.M., Compton, T., Bailey, R.M., Van Den Bergh, G.D., De Vos, J., Pike, A.W.G., Stringer, C., Saptomo, E.W., Rizal, Y., Zaim, J., Santoso, W.D., Trihascaryo, A., Kinsley, L., Sulistyanto, B., 2017. An early modern human presence in Sumatra 73,000–63,000 years ago. Nature 548, 322–325. https://doi.org/10.1038/nature23452.
Westley, K., Dix, J., 2006. Coastal environments and their role in prehistoric migrations. J. Marit. Archaeol. 1, 9–28. https://doi.org/10.1007/s11457-005-9004-5.
White, J.C., Penny, D., Kealhofer, L., Maloney, B., 2004. Vegetation changes from the late Pleistocene through the Holocene from three areas of archaeological significance in Thailand. Quat. Int. 113, 111–132. https://doi.org/10.1016/j.quaint.2003.09.001.
Wurtz, C.B., 1955. The American Camaenidae. Proc. Acad. Natl. Sci. Phila. 107, 99–143.
Xiao, W.L., 1989. Study on the bionomics of *Camaena cicatricosa*. J. Jinan Univ. (Natural Sci. Med. Ed.) 1, 46–52.
Yanes, Y., Fernández-Lopez-de-Pablo, J., 2017. Calibration of the stable isotope composition and body size of the arid-dwelling land snail *Sphincterochila candidissima*, a climatic archive abundant in Mediterranean archaeological deposits. The Holocene 27, 890–899. https://doi.org/10.1177/0959683616675943.
Yanes, Y., Delgado, A., Castillo, C., Alonso, M.R., Ibáñez, M., De la Nuez, J., Kowalewski, M., 2008. Stable isotope ($\delta^{18}O$, $\delta^{13}C$, and δD) signatures of recent terrestrial communities from a low-latitude, oceanic setting: endemic land snails, plants, rain, and carbonate sediments from the eastern Canary Islands. Chem. Geol. 249, 377–392. https://doi.org/10.1016/j.chemgeo.2008.01.008.
Yanes, Y., Romanek, C.S., Molina, F., Cámara, J.A., Delgado, A., 2011. Holocene paleoenvironment (~7200–4000 cal BP) of the Los Castillejos archaeological site (SE Spain) inferred from the stable isotopes of land snail shells. Quat. Int. 244, 67–75. https://doi.org/10.1016/j.quaint.2011.04.031.
Yanes, Y., Izeta, A.D., Cattaneo, R., Costa, T., Gordillo, S., 2014. Holocene (4.5–1.7 cal. kyr BP) paleoenvironmental conditions in central Argentina inferred from entire-shell and intra-shell stable isotope composition of terrestrial gastropods. The Holocene 24, 1193–1205. https://doi.org/10.1177/0959683614540959.
Yapp, C.J., 1979. Oxygen and carbon isotope measurements of land snail shell carbonate. Geochim. Cosmochim. Acta 43, 629–635. https://doi.org/10.1016/0016-7037(79)90170-4.
Yuan, D., Cheng, H., Edwards, R.L., Qing, J., Lin, Y., Wang, Y., Wu, J., 2004. Timing, duration, and transitions of the Last Interglacial Asian monsoon. Science 304, 575–578. https://doi.org/10.1126/science.1091220.
Zanchetta, G., Leone, G., Fallick, A.E., Bonadonna, F.P., 2005. Oxygen isotope composition of living land snail shells: data from Italy. Palaeogeogr. Palaeoclimatol. Palaeoecol. 223, 20–33. https://doi.org/10.1016/j.palaeo.2005.03.024.
Zheng, Z., Lei, Z.Q., 1999. A 400,000 year record of vegetational and climatic changes from a volcanic basin, Leizhou Peninsula, southern China. Palaeogeogr. Palaeoclimatol. Palaeoecol. 145, 339–362. https://doi.org/10.1016/S0031-0182(98)00107-2.